

Chris Barlow

Department of Materials Science
and Engineering,
University of Washington,
Seattle, WA 98195

Vipin Kumar

Department of Mechanical Engineering,
University of Washington,
Seattle, WA 98195

Brian Flinn

e-mail: BFLINN@U.WASHINGTON.EDU

Rajendra K. Bordia

Department of Materials Science
and Engineering,
University of Washington,
Seattle, WA 98195

John Weller

Department of Mechanical Engineering,
University of Washington,
Seattle, WA 98195

Impact Strength of High Density Solid-State Microcellular Polycarbonate Foams

The effect of density (relative densities 0.33 to 0.90) on the impact behavior of microcellular polycarbonate (PC) was investigated. Cell size and foaming gas content were also considered. Flexed-beam Izod impact tests were conducted and the impact strength of these foams appears to be a strong function of both density and cell size. The impact strength was observed to improve over the unprocessed polycarbonate's impact strength for foams with relative densities of 60 percent and above. In terms of cell size, the impact strength increased with increasing cell size at a given density.

[DOI: 10.1115/1.1339004]

Introduction

The question raised by Sue et al. [1] of whether or not microcells are effective in toughening of polycarbonate (PC) has recently been answered in a study by Collias et al. [2] Collias et al. found in PC microcellular foams that the maximum load and impact toughness, measured in sharply notched Charpy impact tests, increased with cell size for cell sizes and densities ranging from 5–45 μm and 97–72 percent relative density. All foams exhibited higher maximum loads and toughness than neat PC. They hypothesized that the microcells induced a brittle-to-ductile transition by relieving the triaxial stress conditions in front of the crack tip.

The above results are promising to microcellular processors, especially where the governing design criteria is impact strength; however, Collias et al. [2] failed to discern whether or not the observed increase in impact strength is dominated by either of the primary foam microstructural variables: density or cell size. In addition, it has been shown by Seeler and Kumar [3], that residual foaming gas trapped in the matrix can have a strong effect on the mechanical behavior. Therefore, the objective of this work is to ascertain the effects of density, cell size and residual gas content on the impact strength of solid-state microcellular PC foam. This study takes advantage of the microcellular polycarbonate-carbon dioxide (PC-CO₂) system which has the ability to produce constant density foams with a variation in cell size (Kumar and Weller [4], Weller [5]).

In the process used to produce microcellular foams, the highest temperature in the entire process is in the neighborhood of glass-transition temperature (T_g) of polycarbonate. This is in contrast to the conventional foam extrusion process in which the polymer is melted. To underscore this fundamental difference, the foams produced by the process in this paper are termed "solid state foams."

The cell walls of the solid state foams are expected to have a substantial amount of biaxial orientation as bubbles grow and stretch the polymer in the rubbery state. By comparison, the cell walls of the melt-extruded foams are not expected to have as high a degree of biaxial orientation. For this reason, for a given foam density, the solid-state foams are expected to have improved mechanical properties compared to conventional melt-extruded foams.

Experimental

The polycarbonate used in this study is General Electric's Lexan 9034. This polycarbonate has a published T_g of 150°C and a density of 1.2 g/cm³. Samples measuring 7.6 cm×7.6 cm were cut from the 3.00 mm thick Lexan sheet. These samples were then foamed as described by Kumar and Weller [4]. First, the samples were saturated with CO₂ in a pressure vessel at a temperature of 25°C. The specified pressure and temperature the samples were exposed to will hereafter be referred to as saturation pressure and saturation temperature. The saturation pressure and saturation temperature were regulated to ± 0.1 Mpa and $\pm 1^\circ\text{C}$, respectively, using the University of Washington Pressure Vessel Control System (Holl [6]). As soon as the samples reached their saturation limit (i.e., no more CO₂ could be absorbed by the sample), they were removed from the pressure vessel and allowed to desorb CO₂ for 5 minutes. The samples were then immersed in a heated glycerin bath, and held there for a length of time allowing the samples to foam. To ensure that the foams remained flat, the samples were constrained between spring loaded sheets of perforated aluminum; the sheets were perforated to ensure uniform heat transfer during foaming and the sheets were spring loaded to allow for sample expansion, but not warpage. The temperature at which the glycerin bath was heated to shall be called the foaming temperature. The temperature of the glycerin bath was controlled by a Haake N3 circulator and temperature control system. All samples were allowed to foam for 10 minutes, after which they

Contributed by the Materials Division for publication in the JOURNAL OF ENGINEERING MATERIALS AND TECHNOLOGY. Manuscript received by the Materials Division July 7, 1999; revised manuscript received September 19, 2000. Associate Editor: C. Brinson.

Table 1 Processing conditions, densities and relative densities for Izod impact specimens used in this study. All samples were saturated at saturation pressure of 4 MPa and saturation temperature of 25°C.

Foaming temperature (°C)	Foaming density (g/cm ³)	Relative density	Cell Size (μm)
70	1.07	0.90	4.34
80	0.96	0.81	5.09
90	0.85	0.71	6.96
100	0.74	0.62	6.94
110	0.62	0.52	7.73
120	0.51	0.43	7.18
130	0.39	0.33	8.97

Table 2 Processing conditions, relative densities and cell sizes of foamed samples used to determine the effect of cell size on Izod impact strength. All samples saturated at 25°C.

Saturation pressure (MPa)	Foaming temperature (°C)	Relative Density	Cell size (μm)
1	127.1	0.71	18.05
2	112.1	0.72	12.60
3	100.2	0.72	8.91
4	90.4	0.71	7.56

were removed from the foaming bath and immediately quenched in water held at room temperature. All foaming was conducted at atmospheric pressure.

The processing conditions used to produce samples with varying densities are listed in Table 1. Note that all density samples were produced using a saturation pressure of 4 MPa and a saturation temperature of 25°C. In order to determine the effect of residual CO₂ in the foam matrix on the impact strength, the above variable density samples were tested at different times after foaming: 2 weeks, 7 weeks, 4 months, and 3 years. Samples with constant relative density and varying cell sizes were processed under the conditions listed in Table 2. Note that in both Tables 1 and 2, there is a relative density listed; this relative density is the density of the foam divided by the density of the unprocessed material. Samples in Table 2 have a constant relative density of approximately 0.7 and cell sizes ranging from 7.56 μm to 18.05 μm and were tested 49 days (7 weeks) after foaming.

After foaming, specimens were machined out of the 7.6 cm×7.6 cm plaques to ASTM D256-93a [7], Izod test specimen geometry. Notches were cut with a flywheel cutter at high rotational speed (2100 rpm). The notch radius was determined, using optical microscopy, to be 0.08 mm; this is a deviation from ASTM D256-93a, which recommends a notch radius of 0.25 mm. However, since the test is a relative one, a notch radius of 0.08 mm is sufficient. Specimens were tested on a BLI Impact testing machine, model 1231, made by SATEC Systems, Inc. A 2.7 Joule capacity hammer was used. Five specimens were tested at each condition at room temperature.

Finally, the density of all samples was measured according to ASTM D792 [7]. Average cell size for all samples was determined first by taking micrographs of gold coated, freeze fractured specimen using a scanning electron microscopy (SEM), and second, by applying a stereological method proposed by S. A. Saltykov in the 1960's for determining particle size distribution (Underwood [8], Weller [5]). Fracture surfaces of representative impact specimens were also examined in the SEM.

Results and Discussion

Since it's customary in literature on cellular materials to normalize material properties, such as elastic modulus or strength, by the corresponding property for the unprocessed material, some of

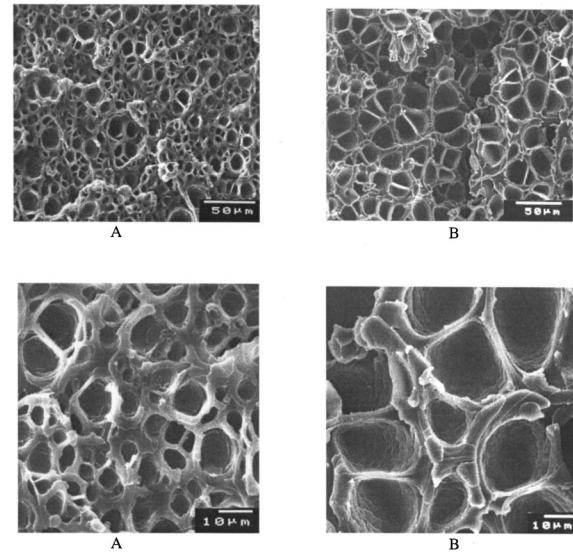


Fig. 1 SEM micrographs of Izod impact fracture surfaces at various densities and cell sizes. (a) Relative density = 0.89, average cell size = 4.3 μm, (b) Relative density = 0.71, average cell size = 18 μm.

the impact properties shown in this section will be shown in a relative fashion. The relative impact strength is then the impact strength of the foam divided by the impact strength of the unprocessed material. Data presented below will first be presented in a raw form showing standard deviation with error bars, then average normalized values will follow.

General Observations. All samples tested in this work fractured in a brittle manner. Examination of the impact specimens revealed no observable macroscopic plastic deformation zones or dimensional changes in any sample. This is to be expected due to the high strain rates associated with impact testing. Representative SEM micrographs of foam fracture surfaces are shown in Fig. 1. These microcellular foams are closed cell foams, with nominally spherical cells. High magnification examination of the fractured cell walls showed no evidence of microplasticity, except for a narrow band, nominally 200 μm wide at the end of the specimen opposite the notch where a plastic hinge developed during the end

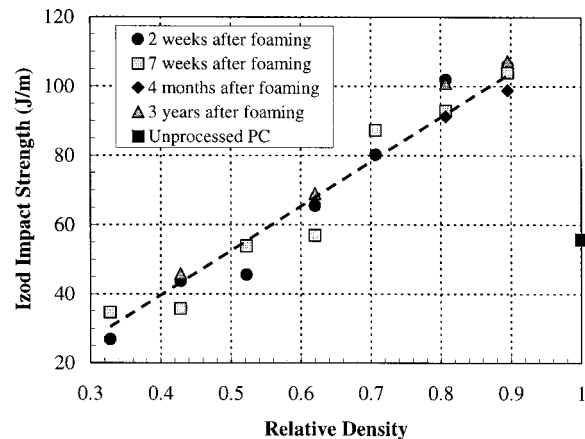


Fig. 2 Izod impact strength as a function of relative density. Note the different samples at different times after foam to determine the effect of foaming gas on impact strength.

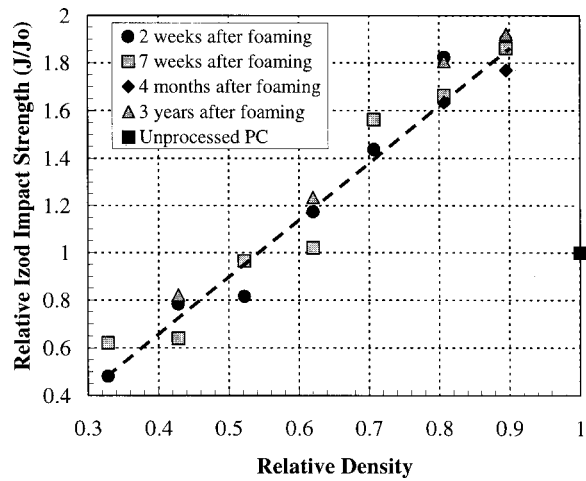


Fig. 3 Relative Izod impact strength as a function of relative foam density

of fracture. The fracture appearance of the cell walls was similar for all samples. Fracture surface roughness increased slightly with increasing cell size.

The Effect of Density. Figure 2 shows the Izod impact strength as a function of relative density for foams with a narrow distribution of cell sizes (4–7 μm). Note that the impact strength is very reproducible for most cases, the variation in strength is less than 5 percent. The impact strength of the foamed samples decreased in a linear manner with density. Surprisingly, foams with relative densities of 0.62 and above all demonstrate an improvement in impact strength, compared to the unprocessed samples (relative density = 1.0). Figure 2 shows the highest impact strength of 105 J/m was achieved at a relative density of 0.9, whereas the unprocessed PC had an impact strength of 55 J/m. This behavior is also seen in Fig. 3, which shows the relative Izod impact strength as a function of relative density. From this figure, it is seen that the 0.89 relative density samples have an impact strength almost 1.9 times that of the unprocessed PC. We see that even with nearly 68 percent reduction in density, the Izod impact strength only drops approximately 50 percent from that of the unprocessed PC. These results are promising for the microcellular processor, considering almost a 40 percent density reduction can be obtained while maintaining the impact strength of the unpro-

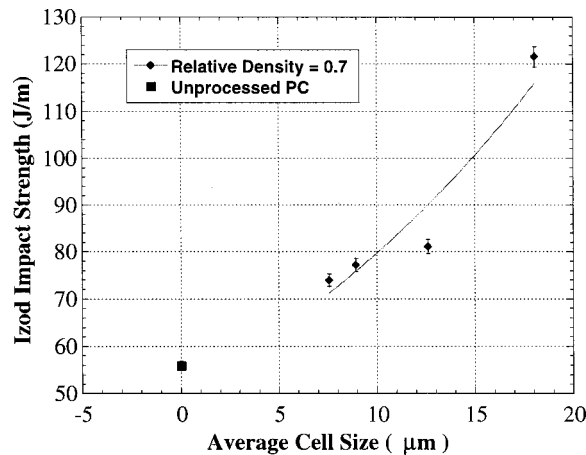


Fig. 4 Izod impact strength as a function of average cell size. Note that all cell size samples in this plot have a relative density = 0.7. A line has been drawn through the data to aid the eye.

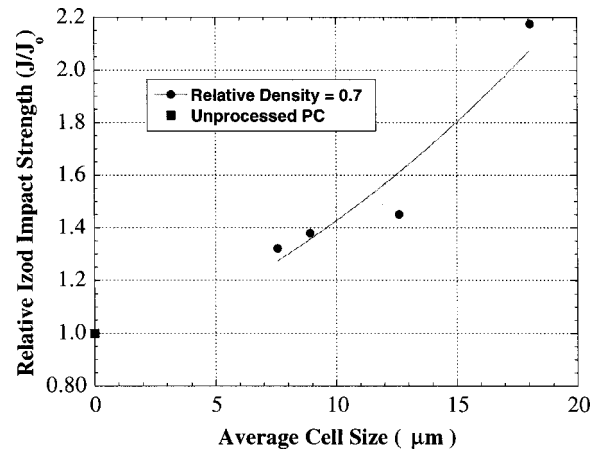


Fig. 5 Relative Izod impact strength as a function of average cell size. Note that all cell size samples in this plot have a relative density = 0.7. A line has been drawn through the data to aid the eye.

cessed PC. To study the effect of residual gas in the foam matrix, samples were tested at different times after foaming since it's been observed that residual CO_2 in the foam continues to desorb at room temperature (Weller [5]). The effect of residual CO_2 in the foams appears to be negligible after 2 weeks of desorption, since the results for those samples tested from 2 weeks – 3 years after foaming are within experimental scatter. This is in accordance with Collias et al. [2] findings; they found that residual nitrogen in the foam matrix did not affect the maximum load and total energy per unit thickness after 10 days.

The Effect of Cell Size. Figures 4 and 5 show the Izod impact strength and relative Izod impact strength as a function of average cell size, respectively. In both plots, at a constant relative density equal to 0.7, the impact strength is observed to increase with increasing cell size. The highest impact strength observed occurs at a cell size of 18.05 μm with a value of 122 J/m. This is almost 2.2 times that of the unprocessed polycarbonate as shown in Fig. 5.

Using neat laminated tape specimens and rubber toughened systems, many authors (Collias and Baird [2], Wu [9], van der Sanden et al. [10,11]) have proposed a critical ligament thickness for polymers below which the ligaments yield and above which they craze. For this study, the ligament thickness is estimated by assuming a simple cubic lattice as seen in Fig. 6. Then using Eq. (1.1) which relates the volume fraction of the pores, V_p , to the

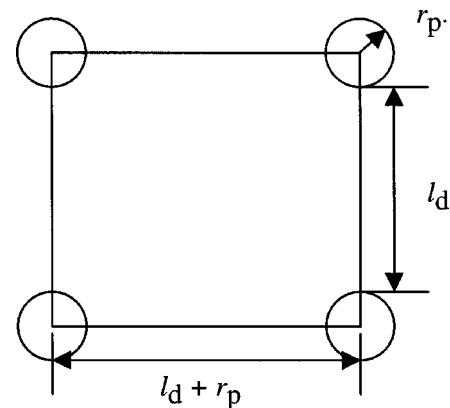


Fig. 6 Simplified model of pore structure used to calculate cell wall thickness

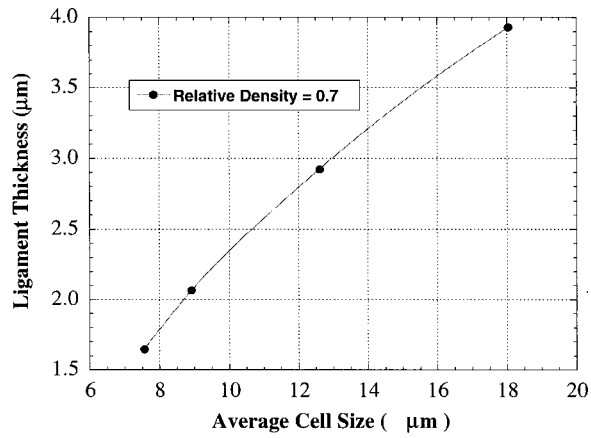


Fig. 7 Calculated ligament thickness as function of cell size for relative density = 0.7. A line has been drawn through the data to aid the eye.

radius of the pores, r_p , the ligament thickness (cell wall thickness), l_d , and relative density, D , we can derive Eq. (1.2) which shows the ligament thickness, l_d , as a function of relative density, D , and radius of the pores, r_p .

$$V_p = \frac{(4/3\pi)r_p^3}{(2r_p + l_p)^3} = 1 - D \quad (1.1)$$

$$l_p = \frac{(4/3\pi)^{1/3}r_p}{(1-D)^{1/3}} - 2r_p \quad (1.2)$$

The calculated ligament thickness is plotted against average cell size in Fig. 7 and is shown to increase with increasing cell size. Thus, plotting the Izod impact strength as a function of ligament thickness, as shown in Fig. 8, demonstrates that the impact strength increases with increasing ligament thickness just as the impact strength increases with average cell size. These results are contrary to trends reported in conventional foams and rubber toughened materials.

The cell size (and hence ligament thickness) dependence of the impact strength is important and a new result obtained from this work. The following observations are important to understand this behavior. First, the fracture mode is brittle in all cases as shown in Fig. 1. This implies that even for the smallest cell size, the local crazing stress is higher than the yield stress. It should be noted

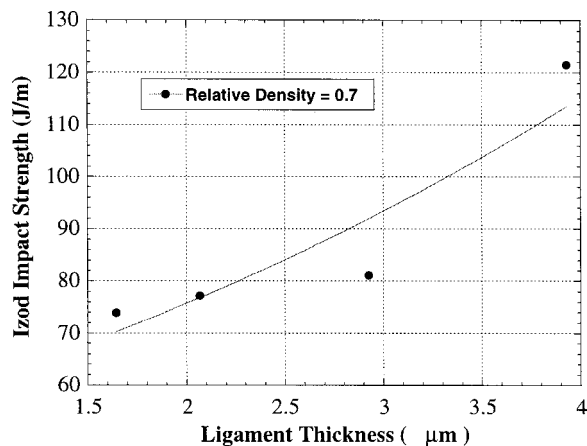


Fig. 8 Izod impact strength as function of calculated ligament thickness from Eq. (1.2). A line has been drawn through the data to aid the eye.

that if shearing was the dominant mode of failure, then impact strength should decrease as ligament size increases as shown by Wu [9] (contrary to the observed results). We therefore hypothesize two possible mechanisms for the observed increase in impact strength with increased ligament thickness. 1) Since a flexed-beam impact test such as the Izod impact test places the test specimen in bending, the bending stress becomes very important in such brittle fractures as seen in these tests. The effective resistance to bending or the moment of inertia of the smaller ligaments is less than the larger ligaments when placed in bending. This then would explain the increase in impact strength with larger ligaments; these larger ligaments provide a greater resistance to bending because they have a higher bending moment of inertia. 2) Although the fracture is predominately brittle, some plasticity occurs in front of the crack tip. The plastic zone size ahead of the crack tip will be limited by the thickness of the ligament for thin cell walls. As the cell wall thickness increases with cell size, a larger plastic zone could develop and increase the energy absorbed during fracture. These hypotheses are not exclusive and need to be tested by conducting tensile tests under equivalent conditions (high strain rate or low temperature). Since Izod impact tests induce strain rates 1000–10,000 times greater than those encountered in a typical tensile test, the polycarbonate experiences brittle fractures (brittle fracture surfaces are present). An equivalent method to induce brittle fracture in tensile tests would be to lower the temperature.

Conclusions

Microcellular polycarbonate foams were produced with a controlled range of cell sizes and densities. The Izod impact strength of unprocessed and foamed polycarbonate was measured at different densities, cell sizes and gas desorption times.

- 1 The Izod impact strength of microcellular foams was greater than unprocessed PC for relative densities over 60 percent.
- 2 The Izod impact strength of foams increased with density.
- 3 Cell wall thickness increased with cell size at a given foam density.
- 4 The Izod impact strength increased with cell size at a given foam density.
- 5 The effect of residual CO₂ on the impact strength of Polycarbonate foams appears to be negligible after 2 weeks of desorption.

The density of polycarbonate can be reduced by up to 40 percent without any reduction in the impact strength relative to solid polycarbonate. Thus, in applications where impact strength governs the design, it is possible to use microcellular polycarbonate foams and realize considerable material savings. The observed increase in impact strength with increasing cell size may be related to ligament size: The thicker cell walls provide a greater volume for plastic deformation and/or a higher moment of inertia to the bending that is experienced during the impact test.

Acknowledgments

This research was primarily supported by the UW-Industry Cellular Composites Consortium. Bordia acknowledges partial support for this research from the National Science Foundation under Grant Number DMR-NYI-9257827 and from the DuPont Young Professor Award. This support is gratefully acknowledged.

References

- [1] Sue, H. J., Huang, J., and Yee, A. F., 1992, "Interfacial Adhesion and Toughening Mechanisms in an Alloy of Polycarbonate/Polyethylene," *Polymer*, **33**, No. 22, pp. 4868–4871.
- [2] Collias, D. I., Baird, D. G., and Borggreve, R. J. M., 1994, "Impact Toughening of Polycarbonate by Microcellular Foaming," *Polymer*, **35**, No. 18, pp. 3978–3983.

- [3] Seeler, K. A., and Kumar, V., 1995, "Decoupling the Effects of the Matrix Properties and Foam Structure on the Mechanical Properties of Microcellular Foam by Sub- T_g Annealing," *J. Reinf. Plast. Compos.*, **14**, pp. 1054–1068.
- [4] Kumar, V., and Weller, J. E., 1994, "Production of Microcellular Polycarbonate Using Carbon Dioxide for Bubble Nucleation," *ASME J. Ind.*, **116**, pp. 413–421.
- [5] Weller, J. E., 1996, "The Effects of Processing and Microstructure on the Tensile Behavior of Microcellular Foams," Ph.D. thesis, Dept. of Mechanical Engineering, University of Washington, Seattle.
- [6] Holl, M., 1994, "The University of Washington Saturation Vessel Pressure and Temperature Control System," Cellular Composites Consortium Report #8, University of Washington, Seattle, WA.
- [7] Annual Book of ASTM Standards, 1996, Vol. 8.01, American Society for Testing and Materials, Philadelphia, PA, pp. 1–18, 293–296.
- [8] Underwood, E. E., 1970, *Quantitative Stereology*, Addison-Wesley, Reading, MA.
- [9] Wu, S., 1987, "A Generalized Criterion for Rubber Toughening: The Critical Matrix Ligament Thickness," *Polym. Prepr. (Am. Chem. Soc. Div. Polym. Chem.)*, **28**, No. 2, pp. 179–80.
- [10] van der Sanden, M. C. M., Meijer, H. E. H., and Lemstra, P. J., 1993, "Deformation and Toughness of Polymeric Systems: 1. The Concept of a Critical Thickness," *Polymer*, **34**, No. 10, pp. 2948–2154.
- [11] van der Sanden, M. C. M., Meijer, H. E. H., and Tervoort, T. A., 1993, "Deformation and Toughness of Polymeric Systems: 2. Influence of Entanglement Density," *Polymer*, **34**, No. 14, pp. 2961–2170.